Optimization of Weld Bead Geometry for Flux Bounded Tungsten Inert Gas Welding of 316L Stainless Steel

D.P. Pandya* and A.D. Badgujar

School of Engineering and Technology, Navrachana University, Vasna Bhayli Road, Vadodara- 391410, Gujarat, India

Received:13 December 2019, Revised:11 February 2020, Accepted: 13 February 2020, Published: 28 February 2020

*Corresponding Author: dipalip@nuv.ac.in

Abstract

Tungsten Inert Gas (TIG) welding process is used to weld variety of materials, however due to its less penetration and low productivity, Activated TIG (A-TIG) welding process has been introduced. A-TIG welding process overcomes demerits of TIG welding process but high amount of slag formation is being observed on weld bead surface as molten flux get mixed with base metal. Flux Bounded Tungsten Inert Gas (FB-TIG) is variant of A-TIG welding process which gives high penetration and also conquers the demerits of A-TIG welding process. To achieve constant welding speed and arc length during autogeneous welding experimental set up is developed. This paper presents the effect of activated oxide fluxes such as Al_2O_3, ZnO and TiO_2 on weld bead geometry of SS316L plate. The maximum penetration is reported with TiO_2 flux. Box-Behken design matrix is used to design the experiments and influence of process variables such as welding current, welding speed, arc length on weld bead geometry of SS 316L plate. The process variables are optimized the by Multi-Objective Optimization on the basis of Ratio Analysis (MOORA) as this method proved to be a robust domination over other multi-objective optimization. Maximum weld penetration depth of 5.56 mm has been achieved with desired weld bead quality with optimized process parameters.

Keywords

A-TIG, FB-TIG welding, Flux, MOORA

Introduction

Austenitic stainless steels are widely used in heat exchangers, aircraft engine parts and furnace parts due to its excellent properties like high corrosion resistance, high strength and ductility[1]. It contains minimum 10.5 % chromium with addition of other elements such as C, Mo, Ni, Cu, Ti, W, N, Mn[2,4]. From total volume 50% stainless steel products is made from austenitic group of stainless steels[1]. TIG is popular process among all welding processes to weld verity of materials. However due to less penetration in single pass and edge preparation reduce the productivity[5]. A-TIG welding process successfully increased the weld penetration more than 300% compared to TIG welding[6,7]. In A-TIG welding flux applied at the weld area which offers the high resistance to arc and becomes conductive only at high temperature. As fraction of the arc energy is used to melt and vaporize the flux, the process effectiveness decreases[8]. Also activated TIG weld bead contain the high amount of slag which is affect the welds quality[9].

These short comings of A-TIG process can be overcome by novel approach of FB-TIG proposed by Sire and Marya[10]. In FB-TIG welding process flux is applied on either side of weld centerline leaving the narrow space of metal as shown in figure1[8]. In case of FB-TIG welding arc directly comes in contact with base metal due to this FB-TIG welding eliminate the adverse effect of A-TIG welding.

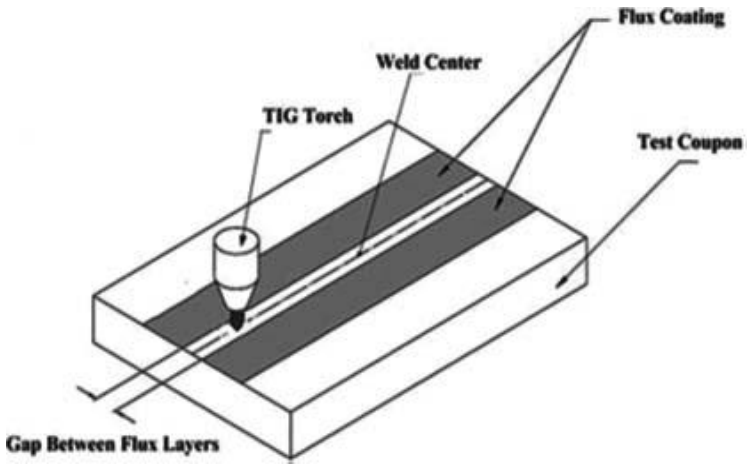

Figure 1: A schematic diagram of flux bounded TIG welding[8]

Mechanisms of improved penetration in A-TIG welding have been proposed are also applicable to FB-TIG welding. The first mechanism identified by Heiple (1982) is Gibbs Merangoni effect[11]. In merangoni effect the direction of fluid flow depends on surface tension

gradient of weld pool, due to surface active elements (flux) surface tension gradient become negative to positive with temperature gradient and create the deeper penetration[12]. In case of FB-TIG welding by reducing the flux gap concentration of surface active elements increases in weld pool and thereby create the inward flow in weld pool[13]. Second mechanism is arc constriction, discovered by Howse and Lucas in 2000[14]. In this phenomena vaporized flux capture the electron from outer region of arc, forms the arc more constrict and there by create the inward flow in weld pool[15,16]. The third prime mechanism is insulating effect which only observed in FB-TIG welding[13]. In FB –TIG welding oxide flux coating on either side of the weld centerline act as insulating barrier so during the welding electron choose the least resistive path and forms the arc more constrict[13]. Due to insulating effect improvement in penetration is observed by Vilarinho et al. in FB-TIG welding[17]. Increase in the flux gap, penetration capability is decreases reported by Ding et al.[18] and Ruckert et al.[8]. FB-TIG welding on AISI 304L is performed, reveals that SiO_2 flux effect weld penetration more compare to TiO_2 and Cr_2O_3[19]. Mechanical properties were observed in A-TIG and FB-TIG welding in aluminum and alloy steel[20,21]. However efficient investigation on weld bead morphology is not presented in published literature.

Experimental Investigation

Austenitic stainless steel 316L was used for experimental study whose chemical composition is listed in Table 1. The 6 mm thick plates cut to 100 mm length 40 mm width for butt welding. To study the effect of variables in FB-TIG welding, it is required to achieve the different welding speed and arc length during the autogeneous welding. To achieve the desired result welding fixture has been developed as shown in figure 2.

316L	Cr	Ni	C	Si	Mn	P	S	Mo	Fe
	24.11	20.7	0.046	0.44	1.47	0.016	0.01	0.07	Max Balance

Table 1: Chemical composition of 316l L stainless steel plate

To examine the influence of oxide flux such as Titanium Dioxide (TiO_2), Zinc Oxide (ZnO) and aluminum oxide (Al_2O_3) on 316L mixed with acetone to obtain the paint like consistency. Before welding plates are machined on milling machine to remove the air gap between butt joint. Plate surface is cleaned with acetone in order to eliminate the surface

impurities. Before welding uniform thickness 0.15 mm flux is spread with paint brush on either side of weld line by keeping the 4 mm gap on surface as shown in figure 3.

Figure 2: Welding Fixture

Figure 3: Application of flux before welding

Operating welding parameters are given in table 2 to perform the autogeneous TIG and FB-TIG welding. To examine the influence of flux, welding current, speed and arc length are kept 140 Amps, 135 mm/min and 2 mm respectively, these process variables are selected from literature survey. Flux gap varies between 2 to 7 mm. In present study flux gap is kept 2 mm as Venkatesan et al.[19] has reported that increase in flux gap weld penetration start to reduce.

Arc length	2mm
Shielding gas flow rate	12 l/min
Shielding gas	Argon,
Vertex angle of electrode	45^0
Welding electrode	Thoriated Tungsten (EWTh-2) diameter (d) 2.5 mm
Conical length of electrode	3 mm
Torch angle	90^0
Nozzle diameter	8 mm
Flux width	12 mm
Flux gap	2 mm

Table 2: Autogeneous Welding parameters for TIG and FB-TIG welding

After welding process, the cross section of weldment was polished and etched in 100ml of hydrochloric acid with 5gm of copper sulphate mixture. Weld bead macrostructures is observed. Higher depth to width ratio was observed with FB-TIG process compare to

conventional TIG welding process. The result indicated that maximum penetration was achieved in TiO_2 flux as shown in figure.4. Therefore, in the present study TiO_2 flux was used for further experiments.

TIG Weld FB –TIG with ZnO FB-TIG with Al_2O_3 FB-TIG with TiO_2

Figure 4: Weld profile of the TIG and FB-TIG weld beads formed with and without ZnO, Al_2O_3 and TiO_2 oxide flux.

Three factorial three level Box-Behnken design (BBD) approach is adopted to acquire the correlation between the variables (welding current, welding speed, arc length) and responses (bead width and penetration). The variables level was coded as -1 (low), 0 (central point) and 1 (high) as shown in table 3. Trial experiments were performed to identify the range of process variables. At high welding current and minimum welding current condition weld pool become wider as shown in figure 5(a). With low welding current and high welding speed very low penetration was observed as shown in figure 5(b). It was observed that optimum penetration to bead width was achieved with average value of welding current and speed as shown in figure 5(c).

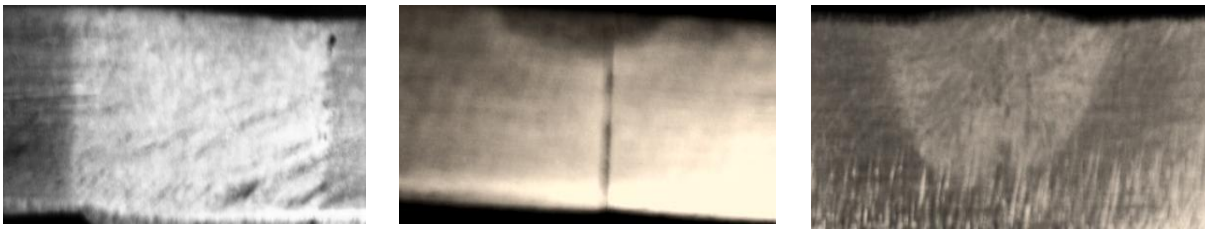

(a) (b) (c)

Welding current : 250 A, Welding speed 80 mm/min

Welding current : 120 A, Welding speed 200 mm/min

Welding current : 150 A, Welding speed 140 mm/min

Figure 5 : Weld profile with TiO_2 flux and at different welding parameters

From the above results working range of process variables were identified as shown in table3.

Variables	Factor Levels		
	-1	0	1
Welding current (Ampere)	120	150	180
Welding speed (mm/min)	120	140	160
Arc length (mm)	1	2	3

Table 3: Welding variables and levels for FB-TIG welding

In the present study experiments were conducted based on BBD technique and analyzed the depth of penetration and bead width, results shown in table 4.

Trial	**Input Parameters**			**Responses**		
	Welding Speed (mm/min)	**Arc length (mm)**	**Current (Ampere)**	**Penetration (P)(mm)**	**HAZ width (W) (mm)**	**Aspect ratio (P/W)**
1	120	1	150	4.22	5.82	0.72
2	160	1	150	3.93	6.43	0.61
3	120	3	150	4.61	6.52	0.70
4	160	3	150	3.42	6.11	0.55
5	120	2	120	3.54	5.86	0.60
6	160	2	120	2.24	6.32	0.35
7	120	2	180	3.87	6.29	0.61
8	160	2	180	3.65	6.30	0.57
9	140	1	120	2.43	5.13	0.47
10	140	3	120	2.17	4.92	0.44
11	140	1	180	3.64	7.22	0.50
12	140	3	180	3.48	6.85	0.51
13	140	2	150	5.56	6.22	0.89

Table 4: Box Behken design matrix and results

FB-TIG weld metal microstructure observed under 20x magnification. The weld profile is measured in terms of D/w ratio which is more desirable if it near to unity. Maximum D/w ratio was reported with experiment 13 (welding current 150 amps, arc length 2 mm, welding speed 140 mm/min),as shown in table 4.

Optimization of process variables

In current study multi objective optimization is carried out by MOORA method as this method prove to be a robust domination over other methods[22].The MOORA method response matrix presenting the performance of different alternative solution with respect to all objectives [23-25].

$$X = \begin{bmatrix} X_1(1) & X_1(2)... & X_1(n) \\ X_2(1) & X_2(2)... & X_2(n) \\ X_m(1) & X_m(2)... & X_m(n) \end{bmatrix} \qquad \text{-------(1)}$$

where m is the number of alternatives, and n is the number of objectives.

The ratio system which is part of MOORA is used in this study. In this method each performance of an alternative on an objective is compared to a denominator which is a representative for all the alternatives linking to that objective [24]. This ratio can be articulated as below:

$$X_{ij}{}^{a} = X_{ij} / \sqrt{\sum_{i=1}^{m} X_{ij}{}^{2}} \qquad \text{---------(2)}$$

where X_{ij} is a dimensionless number, belongs to the interval [0,1] representing the normalized performance of i[th] alternative on j[th] objective [24].

In multi-objective optimization, the case with maximization these normalized performances are added for favorable attributes and with minimization case it is subtracted for unfavorable attributes. The optimization problem converts:

$$Y_i = \sum_{j=1}^{g} X_{ij}{}^{a} - \sum_{j=g+1}^{a} X_{ij}{}^{a} \qquad \text{---------(3)}$$

where g is the number of attributes to be maximized, a is the number of attributes to be minimized, and Y_i is the normalized assessment value of i[th] alternative with respect to all objectives[24]. In some cases, its often observed that some attributes are more important than the others. In order to give more importance to that attribute, it is multiplied with its

corresponding constant[25]. The modified question 3 becomes as follows:

$$Y_i = \sum_{j=1}^{g} W_j \times X_{ij}{}^{a} - \sum_{j=g+1}^{n} W_j \times X_{ij}{}^{a} \qquad \text{--------(4)}$$

where W_j is the weight of j[th] attribute, which can be determined by Analytic Hierarchy Process (AHP) or entropy method. An ordinal ranking of Yi shows the final preference. Thus, the best alternative has the maximum Yi value, while the worst alternative has the minimum Yi value.

In FB-TIG welding to optimize weld penetration, bead width and aspect ratio MOORA method is implemented. Weightage of various responses are 0.45,0.10 and 0.45 for penetration, bead width and aspect ratio respectively. The normalized performance values of each attributes were obtained using equation 2, shown in table 5. Based on these score and acquired weightage of each response, normalized assessment value of each attributes are calculated using equations 4. The outcome of the MOORA method, provides ranking of each attributes based on the normalized assessment value as shown in table 5.

Trial No.	Penetration (mm)	Bead width (mm)	Aspect ratio	$\bar{Y}$	Rank
1	0.2720	0.2429	0.2900	0.2286	3
2	0.2533	0.2683	0.2457	0.1977	4
3	0.2971	0.2721	0.2820	0.2334	2
4	0.2204	0.2550	0.2215	0.1734	8
5	0.2281	0.2445	0.2417	0.1870	6
6	0.1444	0.2637	0.1410	0.1020	13
7	0.2494	0.2625	0.2457	0.1966	5
8	0.2352	0.2629	0.2296	0.1829	7
9	0.1566	0.2141	0.1893	0.1343	11
10	0.1399	0.2053	0.1772	0.1222	12
11	0.2346	0.3013	0.2014	0.1661	9
12	0.2243	0.2859	0.2054	0.1648	10
13	0.3583	0.2596	0.3585	0.2966	1

Table 5: Normalized decision-making matrix and results of multi-objective analysis

Rank of table 5 will help to identify the optimal values of process variables.

Conclusion

Present study reveals that FB-TIG welding with TiO_2 flux provide the higher penetration compare to other two oxide fluxes (ZnO, Al_2O_3) on 316L stainless steel plate. Higher penetration is reported in FB-TIG welding by overcoming the limitation of A-TIG welding which make the process more attractive. Optimized FB-TIG welding process parameters obtained are welding current 150 amperes, welding speed of 140 mm/min and arc length 2 mm, for 6 mm thick SS 316L plate by MOORA method. These combinations of process parameter obtained penetration 5.56 mm, bead width 6.22mm with maximum aspect ratio 0.89.

References

1. Brinkman C. R. & Garvin, H.W.(1979).*Properties of Austenitic Stainless Steels and Their Weld Metals (Influence of Slight Chemistry Variations)*, Retrieved from Google books: https://books.google.co.in/books?id=fTz59UaMuJwC.
2. Umoru L E., Afonja A. A. & Ademodi B. (2008). Corrosion study of AISI 304, AISI 321 and AISI 430 stainless steels in a tar sand digester, *Journal of Minerals & Materials Characterization & Engineering, 7(4).*291-299. DOI: 10.4236/jmmce.2008.74022
3. Otokumpu O.(2013). *Handbook of Stainless Steel*, Avesta Resarch Centre, Avesta. Sweden: Outokumpu Oyj.
4. Davis J. R.(1994). *ASM Specialty Handbook: Stainless Steels*. USA : ASM International
5. Vidyarthy, R.S. & Dwivedi, D.K.(2016) Activating flux tungsten inert gas welding for enhanced weld penetration. *International Journal of Manufacturing Processes*,22, 211-228. https://doi.org/10.1016/j.jmapro.2016.03.012
6. Lucas, W. & Howse, D. (1996). Activating flux - Increasing the performance and productivity of the TIG and plasma processes. *Welding and Metal Fabrication*, 64, 11 – 17.
7. Choudhary, S. & Duhan, R.(2015). Effect of Activated Flux on Properties of SS 304 Using TIG Welding. *International Journal of Engineering*, *28(2)*, 290-295.
8. Rückert, G., Huneau, B. & Marya, S. (2007). Optimizing the design of silica coating for productivity gains during the TIG welding of 304L stainless steel. *Materials and Design*, *28(9)*,2387–2393.

9. Vidyarthy, R.S. & Dwivedi, D.K.(2016) Activating flux tungsten inert gas welding for enhanced weld penetration, *International Journal of Manufacturing Processes, 22,* 211-228. https://doi.org/10.1016/j.jmapro.2016.03.012
10. **S**ire, S. & Marya, S. (2001). New perspectives in TIG welding through flux application FBTIG process. *Proceeding of the 7th International Welding Symposium, Japan welding Society*, 113–118.
11. Heiple,C.R. & Roper J.R. (1982).Mechanism for minor element effect on GTA fusion zone geometry. *Welding Journal, 61 (4),* 97–102.
12. Mills, K.C., Keene, B.J., Brooks, R.F. & Shirali, A. (1998). Marangoni effects in welding. *Philosophical Transactions of the royal society A Mathematical, Physical and Engineering Sciences*,356(1739), 911–925.
13. Jayakrishnan, S. & Chakravarthy, P.(2017). Flux bounded tungsten inert gas welding for enhanced weld performance - A review. *Journal of Manufacturing Processes, 28(1),*116–130. https://doi.org/10.1016/j.jmapro.2017.05.023
14. Howse, D.S. & Lucas, W.(2000). An investigation into arc constriction by active fluxes for TIG (A-TIG).*welding Science and Technology of Welding and Joining,5 (3),*189-193.
15. Skvortsov, E.A.(1998). Role of electronegative elements in contraction of the arc discharge', *Welding International,12(6),*471–475**.**
16. Tanaka, M., Shimizu, T., Terasaki, T., Ushio, M. & Koshiishi, F.(2000). Effects of activating flux on arc phenomena in gas tungsten arc welding. *Science and Technology of Welding and Joining ,5,* 397–402.
17. Vilarinho, L. O., Kumar, V., Lucas, B. & Raghunathan, S. (2009). Investigation of the A-TIG mechanism and the productivity benefits in TIG welding. *Proceedings of 20th international congress of mechanical engineering ABCM*, Gramado, RS, Brazil Cobem.
18. Ding, F. & Yong, H.,(2005). Study on Activating TIG Welding For Aluminium Alloys. *Welding In The World, 49.*
19. Venkatesan, G., Muthupandi, V. & Fathaha, A.B. (2017). Effect of Oxide Fluxes on Depth of Penetration in Flux Bounded Tungsten Inert Gas Welding of AISI 304L Stainless Steel. *Transactions of the Indian Institute of Metals,70 (6),*1455–1462**.** https://doi.org/10.1007/s12666-016-0942-4

20. Santhana Babu, A.V., Giridharan, P.K.,Ramesh Narayanan, P. & Narayana Murty, S.V.S.(2014).Microstructural investigations on ATIG and FBTIG welding of AA 2219 T87 aluminum alloy. *Applied Mechanics and Materials, 592,* 489–493. https://doi.org/10.4028/www.scientific.net/AMM.
21. Maduraimuthu, V., Vasudevan, M., Muthupandi, V., Bhaduri, A.K.& Jayakumar, T. (2012). Effect of activated flux on the microstructure, mechanical properties, and residual stresses of modified 9Cr-1Mo steel weld joints. *Metallurgical and Materials Transactions B,43(1),* 123–132.https://doi.org/10.1007/s11663-011-9568-4
22. Brauers WKM & Zavadskas EK.(2009). Robustness of the multiobjective MOORA method with a test for the facilities sector. *Technological and Economic Development of Economy: Baltic Journal on Sustainability 15*, 352–375. doi:10.3846/1392-8619.2009.15.
23. Brauers WKM, Zavadskas EK, Peldschus F, & Turskis Z.(2008). Multi objective decision-making for road design. *Transport 23*,183–193 https://doi.org/10.3846/1648-4142.2008.23.183-193.
24. Brauers WKM & Zavadskas EK. (2006). The MOORA method and its application to privatization in a transition economy. *Control Cybern 35*,445–469.
25. Brauers W.K.M., Zavadskas E.K.,Turskis Z.&Vilutiene, T. (2008). Multi-objective contractor's ranking by applying the MOORA method. *Journal of Business Economics and Management 9(4),* 245–255,DOI: 10.3846/1611-1699.2008.9.